Defining SSO Power and Characterizing SSO Propagation in Power System with Wind Farms Integration

Na Yang, Wenda Ma, Xitian Wang, *Member*, *IEEE*, Da Xie, *Senior Member*, *IEEE*, Chenghong Gu, *Member*, *IEEE*, Dawei Zhao, *Member*, *IEEE*, Yu Zhang

***Abstract*—This paper studies the characteristics of subsynchronous oscillation (SSO) power propagation in power systems with a large-scale wind farm integration. Based on the instantaneous power theory, a novel definition of SSO power is proposed to characterize its propagation. The SSO power contains both DC power components and AC power components. Utilizing SSO power, SSO propagation is quantitatively studied in single oscillation source systems, and further studied in multiple oscillation sources systems. Theoretical analysis reveals that in addition to the recognized impact of line impedance, power flow also affects SSO power propagation significantly. Hence, propagation impact factor is proposed for the determination of the dominant influencing element. To reveal SSO power propagation paths in a network, shunt coefficients of DC power components and AC power components are expressed respectively. Test cases under different operating conditions and a practical case are carried out to demonstrate analysis and conclusions in this paper.**

***Index Terms*—power system, wind farm integration, SSO power, power propagation, impact factor, shunt coefficient.**

I. Introduction

IT is well known that the emerging type of subsynchronous oscillation (SSO) caused by wind farms integrated power grid has become one important challenge for power system stable operation [1-3]. Studies have shown that SSO may occur when wind turbine generators (WTGs) are connected to series compensations or weak AC networks [4-5].

In 2009, the first WTGs related SSO event appeared in Texas, USA. It was caused by the interaction between the control of doubly-fed induction generator (DFIG) and fixed series compensation, leading to tripping of numerous WTGs and damage to their crowbar circuits [6-7]. In 2015, SSOs, originated from large-scale wind farms in the northern area of Xinjiang, China, propagated to the turbo generators more than 300km away through multiple voltage levels [8-9]. It is thus of great importance to study the propagation characteristics of SSO, which can deepen the understandings of SSO propagation mechanism and provide a basis for the monitoring and control.

The generation mechanism of SSO caused by grid-connected wind farms has been intensively studied in recent years. Research suggests that the intrinsic mechanism of SSO in series compensated DFIG based wind farm systems is the negative damping characteristics of DFIGs at subsynchronous frequencies [10-12]. The oscillations originated from permanent magnet synchronous generator (PMSG) based wind farms can spread to turbo generators in distant grids [5], [13]. This SSO generation is due to the capacitive impedance characteristics with negative resistance of the PMSGs' controllers at subsynchronous frequencies. When PMSGs are connected to weak AC grid, an electrical resonant loop will be formed, and SSO will occur due to the negative damping effect.

Existing literature on the SSO propagation generally concentrates on i) studying the propagation mechanism of SSO [14], ii) defining the concept of subsynchronous power [15-18], iii) identifying the influencing elements of SSO propagation [19] and iv) determining the propagation path of SSO [20]. Gong Y et al. find that the oscillating current propagates along the weakly damped channel in the synchronous generator-based system [14]. The concept of subsynchronous power using conventional power theory based on the average value is proposed in [15]. The defined subsynchronous power is applied to the real-time determination of wind farms contributing to SSO. [16] proposes a framework to identify the origin of SSO through sub/super-synchronous power flows. In terms of instantaneous power definition, Akagi et al. introduced the instantaneous power theory in the early 1980s, based on the instantaneous value, applied to non-sinusoidal circuits and various transition processes [17-18]. Wen Z et al. propose an oscillation propagation factor, obtained only by the system transfer function matrix, which can represent the propagation characteristics of SSO [19]. In [20], the shunt coefficient which can characterize the SSO propagation path is proposed. This

This work was supported in part by the National Natural Science Foundation of China under Grant 51677114 and the Research Project of State Grid Corporation of China under Grant SGTYHT/16-JS-198.

N. Yang, W. Ma, X. Wang, D. Xie are with the Department of Electrical Engineering (the Key Laboratory of Control of Power Transmission and Conversion, Ministry of Education), Shanghai Jiao Tong University, Shanghai 200240, China (e-mail: 2014yangna@sjtu.edu.cn; 1208600492@qq.com; x.t.wang@sjtu.edu.cn; xieda@sjtu.edu.cn).

C. Gu is with the Department of Electronic and Electrical Engineering, University of Bath, Bath BA27AY, UK (e-mail: c.gu@bath.ac.uk).

D. Zhao is with the Renewable Energy Research Center, China Electric Power Research Institute (State Key Laboratory of Operation and Control of Renewable Energy & Storage Systems), Nanjing 210003, China (e-mail: zhaodawei@epri.sgcc.com.cn).

Y. Zhang is with the State Grid Corporation of China, Shanghai 200437, China (e-mail: zhangy@sgcc.com.cn).

coefficient represents the propagation path of subsynchronous current, which is completely determined by system impedance frequency characteristics.

Because SSO has a great impact on the stable operation of wind integrated power systems, further research on SSO propagation mechanism is required. The concept of subsynchronous power proposed by [15] is applied to SSO source detection. This method is easy to implement and requires limited computational burden. However, the AC power components at the subsynchronous and supersynchronous frequencies are not included. The sub/super-synchronous power flows in [16] didn't consider the power generated by the voltages and currents having dissimilar frequencies. In practice, AC power components have a great impact on SSO propagation and thus, they need to be pinpointed in defining SSO power. In terms of elements affecting propagation and propagation paths, previous research only considers system impedance frequency characteristics. In SSO events, long-distance and cross-voltage-level propagation of SSO is obviously beyond traditional cognition, which thinks SSO propagation is a local issue. Besides, oscillation propagation has been previously analyzed only in single oscillation frequency source systems [14-15, 19-20]. The propagation mechanism of multiple oscillation sources considering the coupling effects of different frequency components has not yet been studied.

To fill the research gap, this paper studies the characteristics of SSO power propagation in wind integrated power systems. The novel definition of SSO power including both DC components and AC components is proposed based on the three-phase instantaneous power theory. It also considers the supersynchronous power component in the asymmetrical operation system. By using the fundamental frequency power flow propagation for reference, SSO propagation mechanism is studied from the perspective of power flow and impedance characteristics. Thus, the impact factor and shunt coefficient are proposed to analyzing the propagation of the components in SSO power. Test cases are conducted on systems with single oscillation source and multiple oscillation sources.

The major contribution of this paper is as follows: (1) Considering the AC power component and asymmetrical system operation deepens understandings of SSO power. (2) The SSO propagation characteristic with multiple oscillation sources in wind farms is revealed based on the definition of SSO power. (3) This paper has found that the propagation is affected by both power flow and line impedance characteristics, which is different from the traditional understanding.

The remainder of this paper is organized as follows. Section II defines SSO power with a single oscillation source. Then the expression of SSO power is further studied in Section III. Section IV analyzes elements affecting SSO power propagation and defines the SSO propagation impact factor and propagation shunt coefficient. Section V verifies the obtained conclusions by the theoretical analysis by time-domain simulations. Brief conclusions are drawn in Section VI.

II. The SSO Power with a Single Oscillation Source

A. Building SSO propagation principle model

Based on analyzing post-fault data of SSO events in wind integrated power systems, WTGs, with negative damping effect or external periodic disturbances, output oscillation energy to the system. According to the oscillation energy flow method [21], the component producing energy has a negative contribution to the damping and is considered as the oscillation source. Therefore, the wind farm outputting oscillation energy is simplified as an oscillation source when we building the principle model. Under small disturbance, the oscillation phenomenon will appear in the wind farm, and the oscillation divergence speed is related to system damping. Thus, the influence of system damping is reflected in the equivalent model of the wind farm.

Fig.1. shows two combinations of fundamental and subsynchronous frequency power sources. u_0, i_0 are the fundamental voltage source and current source; u_{SS}, i_{SS} are the subsynchronous voltage source and current source. To express SSO power more concisely, this paper adopts two voltage sources in series in Fig.2.

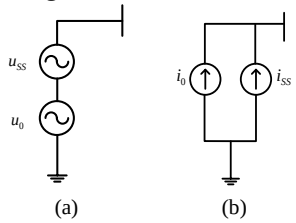

Fig. 1. Combinations of power sources

The principle model of a wind farm integrated system with a single oscillation source is shown in Fig.2. The equivalent wind farm is in the dotted box. The network part is simplified to make the expression of SSO power concise to analyze the SSO propagation characteristics. $u_0(t)$ is the voltage source with frequency ω_0 which represents wind farm outlet fundamental frequency voltage, $u_{SS}(t)$ is the voltage source with frequency ω_{SS}, representing the internal oscillation source of the wind farm. $u(t)$ is the voltage of the system's *PCC*. There are n transmission lines after the PCC. The ending node voltage of the lth line is $u_l(t)$ and the current of the lth line is $i^l(t)$.

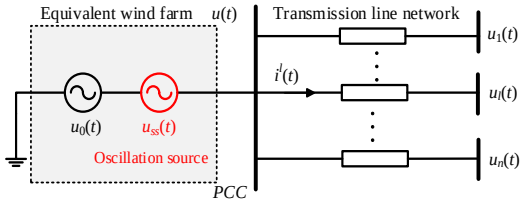

Fig. 2. SSO propagation principle model with a single oscillation source

The three-phase fundamental and subsynchronous frequency voltages are shown in (1). Then, the three-phase fundamental and subsynchronous frequency currents of the lth branch of the system's PCC can be expressed by (2).

$$\begin{cases} u_{a0}(t)=U_0\cos(\omega_0 t+\theta_0) \\ u_{b0}(t)=U_0\cos(\omega_0 t-2\pi/3+\theta_0) \\ u_{c0}(t)=U_0\cos(\omega_0 t+2\pi/3+\theta_0) \end{cases} \begin{cases} u_{aSS}(t)=U_{SS}e^{-\sigma t}\cos(\omega_{SS} t+\theta_{SS}) \\ u_{bSS}(t)=U_{SS}e^{-\sigma t}\cos(\omega_{SS} t-2\pi/3+\theta_{SS}) \\ u_{cSS}(t)=U_{SS}e^{-\sigma t}\cos(\omega_{SS} t+2\pi/3+\theta_{SS}) \end{cases} \quad (1)$$

$$\begin{cases} i_{a0}^{l}(t)=I_0\cos(\omega_0 t+\alpha_0) \\ i_{b0}^{l}(t)=I_0\cos(\omega_0 t-2\pi/3+\alpha_0) \\ i_{c0}^{l}(t)=I_0\cos(\omega_0 t+2\pi/3+\alpha_0) \end{cases} \begin{cases} i_{aSS}^{l}(t)=I_{SS}e^{-\sigma t}\cos(\omega_{SS} t+\alpha_{SS}) \\ i_{bSS}^{l}(t)=I_{SS}e^{-\sigma t}\cos(\omega_{SS} t-2\pi/3+\alpha_{SS}) \\ i_{cSS}^{l}(t)=I_{SS}e^{-\sigma t}\cos(\omega_{SS} t+2\pi/3+\alpha_{SS}) \end{cases} \quad (2)$$

Where U_0, I_0 are the fundamental frequency voltage and current; U_{SS}, I_{SS} are the subsynchronous frequency voltage and current; θ_0, α_0 are the phase angles of fundamental frequency voltage and current; θ_{SS}, α_{SS} are the phase angles of subsynchronous frequency voltage and current; σ is the damping of SSO.

Then, the PCC's three-phase voltages and the *l*th branch's three-phase currents can be obtained in (3).

$$\begin{cases} u_a(t)=u_{a0}(t)+u_{aSS}(t) \\ u_b(t)=u_{b0}(t)+u_{bSS}(t) \\ u_c(t)=u_{c0}(t)+u_{cSS}(t) \end{cases} \begin{cases} i_a^{l}(t)=i_{a0}^{l}(t)+i_{aSS}^{l}(t) \\ i_b^{l}(t)=i_{b0}^{l}(t)+i_{bSS}^{l}(t) \\ i_c^{l}(t)=i_{c0}^{l}(t)+i_{cSS}^{l}(t) \end{cases} \quad (3)$$

B. Expression of instantaneous power

The three-phase instantaneous power at the starting point of the *l*th line is in (4).

$$\begin{cases} p_a(t)=u_a(t)i_a^{l}(t) \\ p_b(t)=u_b(t)i_b^{l}(t) \\ p_c(t)=u_c(t)i_c^{l}(t) \end{cases} \quad (4)$$

Taking phase A instantaneous power as an example, it can be obtained by substituting (3) into (4), where $\omega_{SUP}=\omega_0+\omega_{SS}$ and $\omega_{SUB}=\omega_0-\omega_{SS}$.

$$\begin{aligned} p_a(t)=&U_0I_0\frac{\cos(2\omega_0 t+\theta_0+\alpha_0)+\cos(\theta_0-\alpha_0)}{2}+ \\ &U_{SS}I_0e^{-\sigma t}\frac{\cos(\omega_{SUP}t+\theta_{SS}+\alpha_0)+\cos(\omega_{SUB}t+\alpha_0-\theta_{SS})}{2}+ \\ &U_0I_{SS}e^{-\sigma t}\frac{\cos(\omega_{SUP}t+\theta_0+\alpha_{SS})+\cos(\omega_{SUB}t+\theta_0-\alpha_{SS})}{2}+ \\ &U_{SS}I_{SS}e^{-2\sigma t}\frac{\cos(2\omega_{SS}t+\theta_{SS}+\alpha_{SS})+\cos(\theta_{SS}-\alpha_{SS})}{2} \end{aligned} \quad (5)$$

Mainly the oscillation component contained in the instantaneous active power affects the power grid. When the subsynchronous frequency matches the natural frequency of the shaft modes, resonance is produced, which will reduce the shaft's fatigue life and even endanger the safety of the generator set. Thus, three-phase instantaneous active power is the key research topic on the SSO propagation mechanism.

The instantaneous power theory based on instantaneous value is used to analyze the three-phase instantaneous power in systems with SSO. According to the three-phase instantaneous power theory, three-phase instantaneous active power is the sum of the instantaneous power of each phase, equal to the three-phase instantaneous power, shown in (6). The instantaneous reactive power in each phase does not contribute to the total instantaneous power in the three-phase circuit.

$$\begin{aligned} p(t)&=p_a(t)+p_b(t)+p_c(t) \\ &=\frac{3}{2}U_0I_0\cos(\theta_0-\alpha_0)+\frac{3}{2}U_{SS}I_0e^{-\sigma t}\cos\big((\omega_0-\omega_{SS})t+\alpha_0-\theta_{SS}\big)+ \\ &\quad\frac{3}{2}U_0I_{SS}e^{-\sigma t}\cos\big((\omega_0-\omega_{SS})t+\theta_0-\alpha_{SS}\big)+\frac{3}{2}U_{SS}I_{SS}e^{-2\sigma t}\cos(\theta_{SS}-\alpha_{SS}) \end{aligned} \quad (6)$$

Equation (6) indicates that power components with frequencies of $2\omega_0$, $2\omega_{SS}$ and $(\omega_0+\omega_{SS})$ contained in the single-phase instantaneous power are cancelled because of phase symmetry. The frequency of the subsynchronous power component and the frequency of the subsynchronous voltage or current complement each other, where the sum is ω_0. This result is consistent with analyses on practical SSO event [4].

C. Definition of SSO power

As shown in (6), three-phase instantaneous active power consists of four items, which physical meanings are explained as follows. The first item is the instantaneous active power generated by the fundamental frequency current and voltage, i.e. the rate at which electric field forces, produced by the fundamental frequency voltage, do work on electric charges that make up the fundamental frequency current. The second and third items are the power fluctuation with a frequency of $(\omega_0-\omega_{SS})$, caused by the interaction of fundamental frequency components and subsynchronous frequency components. The second item is the rate at which electric field forces, produced by the subsynchronous frequency voltage, do work on electric charges that make up the fundamental frequency current. The physical meaning of the third item is similar to that of the second item. The fourth item is the active power component completely related to the subsynchronous voltage and current.

This paper defines SSO power in (7) as the last three items in (6) related to the subsynchronous voltage and current generated by the SSO source.

$$\begin{aligned} p_{SS}(t)=&\frac{3}{2}U_{SS}I_0e^{-\sigma t}\cos\big((\omega_0-\omega_{SS})t+\alpha_0-\theta_{SS}\big)+ \\ &\frac{3}{2}U_0I_{SS}e^{-\sigma t}\cos\big((\omega_0-\omega_{SS})t+\theta_0-\alpha_{SS}\big)+ \\ &\frac{3}{2}U_{SS}I_{SS}e^{-2\sigma t}\cos(\theta_{SS}-\alpha_{SS}) \\ =&\,p_{SS\_AC1}(t)e^{-\sigma t}+p_{SS\_AC2}(t)e^{-\sigma t}+p_{SS\_DC}e^{-2\sigma t} \end{aligned} \quad (7)$$

The SSO power includes not only the DC component but also the AC component at $(\omega_0-\omega_{SS})$. When the damping of the SSO component is negative, the magnitude of the SSO power increases. When the damping is equal to 0, the magnitude of SSO power does not change with time. When the damping is positive, the magnitude of SSO power decays to zero.

The above analysis is based on the three-phase symmetrical operating state. When the system is in an asymmetrical operating state, the power components of frequencies $2\omega_0$, $2\omega_{SS}$ and $(\omega_0+\omega_{SS})$ contained in the single-phase instantaneous power cannot be cancelled due to phase asymmetry. There are also supersynchronous components in the SSO power. The case of asymmetrical operation will be analyzed in the following part.

D. SSO Power during Asymmetrical Operation

Unbalanced loads can cause three-phase voltage unbalance. Voltage unbalance is a recognized power quality parameter that measures the asymmetry degree of system operation. Three-phase voltage unbalance factor ε is expressed in (8).

$$\varepsilon=\frac{U_N}{U_P}\times100\%=\frac{\left|\left(\mathbf{U_{0a}}+\mathbf{a}^2\cdot\mathbf{U_{0b}}+\mathbf{a}\cdot\mathbf{U_{0c}}\right)/3\right|}{\left|\left(\mathbf{U_{0a}}+\mathbf{a}\cdot\mathbf{U_{0b}}+\mathbf{a}^2\cdot\mathbf{U_{0c}}\right)/3\right|}\times100\% \quad (8)$$

Where U_N is the RMS value of the negative sequence of the three-phase voltage and U_P is the positive sequence; $\mathbf{U_{0a}}$, $\mathbf{U_{0b}}$ and $\mathbf{U_{0c}}$ are phase voltage vectors; $\mathbf{a}=-1/2+j\sqrt{3}/2$.

Take the power components in the third item of (5) as an example (with frequencies of ω_{SUP} and ω_{SUB}). When the system is in an asymmetrical operating state, they can be expressed by (9) and (10).

$$p_{SUP}(t)=p_{SUPa}(t)+p_{SUPb}(t)+p_{SUPc}(t)$$
$$=\frac{1}{2}I_{SS}e^{-\sigma t}\begin{bmatrix}U_{0a}\cos(\omega_{SUP}t+\theta_0+\alpha_{SS}+\varphi_a)+\\U_{0b}\cos(\omega_{SUP}t+\theta_0+\alpha_{SS}+\varphi_b+2\pi/3)+\\U_{0c}\cos(\omega_{SUP}t+\theta_0+\alpha_{SS}+\varphi_c-2\pi/3)\end{bmatrix} \quad (9)$$

$$p_{SUB}(t)=p_{SUBa}(t)+p_{SUBb}(t)+p_{SUBc}(t)$$
$$=\frac{1}{2}I_{SS}e^{-\sigma t}\begin{bmatrix}U_{0a}\cos(\omega_{SUB}t+\theta_0-\alpha_{SS}+\varphi_a)+\\U_{0b}\cos(\omega_{SUB}t+\theta_0-\alpha_{SS}+\varphi_b)+\\U_{0c}\cos(\omega_{SUB}t+\theta_0-\alpha_{SS}+\varphi_c)\end{bmatrix} \quad (10)$$

Where φ_a, φ_b and φ_c are three-phase voltage phase angle deviations caused by asymmetrical operation. As shown in (9) and (10), the supersynchronous components $p_{SUP}(t)$ are $I_{SS}e^{-\sigma t}$ times of the three-phase negative voltage sequence component. The subsynchronous power component $p_{SUB}(t)$ are $I_{SS}e^{-\sigma t}$ times of the positive sequence component. The magnitude ratio of $p_{SUP}(t)$ to $p_{SUB}(t)$ can be expressed by (11).

$$\frac{|p_{SUP}(t)|}{|p_{SUB}(t)|}=\frac{\left|\left(\mathbf{U_{0a}}+\mathbf{a}^2\cdot\mathbf{U_{0b}}+\mathbf{a}\cdot\mathbf{U_{0c}}\right)\right|}{\left|\left(\mathbf{U_{0a}}+\mathbf{a}\cdot\mathbf{U_{0b}}+\mathbf{a}^2\cdot\mathbf{U_{0c}}\right)\right|}\propto\varepsilon \quad (11)$$

Equation (11) shows that the ratio is proportional to the three-phase voltage unbalance factor ε, which is generally smaller than 4% according to power quality regulation. Therefore, SSO power is dominated by the subsynchronous frequency component during asymmetrical system operation.

III. SSO Power with Multiple Oscillation Sources

The coupling relationship among wind farms with different parameter settings may cause multiple oscillation frequencies in SSO power. This phenomenon may affect the characteristics of SSO power propagation. When there are multiple frequency oscillation sources in the system, assuming that there are n different frequency sources, the three-phase oscillation frequency voltages and currents at the PCC are (12). They are obtained according to the circuit superposition principle.

$$\begin{cases}u_{aSS}(t)=\sum_{k=1}^{n}U_{SSk}e^{-\sigma_k t}\cos(\omega_{SSk}t+\theta_{SSk})\\u_{bSS}(t)=\sum_{k=1}^{n}U_{SSk}e^{-\sigma_k t}\cos(\omega_{SSk}t-2\pi/3+\theta_{SSk})\\u_{cSS}(t)=\sum_{k=1}^{n}U_{SSk}e^{-\sigma_k t}\cos(\omega_{SSk}t+2\pi/3+\theta_{SSk})\end{cases}\quad\begin{cases}i^{l}_{aSS}(t)=\sum_{k=1}^{n}I_{SSk}e^{-\sigma_k t}\cos(\omega_{SSk}t+\alpha_{SSk})\\i^{l}_{bSS}(t)=\sum_{k=1}^{n}I_{SSk}e^{-\sigma_k t}\cos(\omega_{SSk}t-2\pi/3+\alpha_{SSk})\\i^{l}_{cSS}(t)=\sum_{k=1}^{n}I_{SSk}e^{-\sigma_k t}\cos(\omega_{SSk}t+2\pi/3+\alpha_{SSk})\end{cases} \quad (12)$$

Where ω_{SSk} is the kth oscillation source's frequency; U_{SSk}, I_{SSk} are the magnitudes of the kth oscillation source voltage and current; θ_{SSk}, α_{SSk} are the phase angles of the kth oscillation frequency voltage and current; σ_k is the damping of the kth oscillation component.

According to the SSO power definition in Section II, SSO power with n oscillation sources is shown in (13).

$$p_{SSn}(t)=\frac{3}{2}\begin{Bmatrix}\sum_{k=1}^{n}U_0I_{SSk}e^{-\sigma_k t}\cos((\omega_0-\omega_{SSk})t+\theta_0-\alpha_{SSk})+\\\sum_{k=1}^{n}U_{SSk}I_0e^{-\sigma_k t}\cos((\omega_0-\omega_{SSk})t+\alpha_0-\theta_{SSk})+\\\sum_{k=1}^{n}\sum_{j=1}^{n}U_{SSk}I_{SSj}e^{-(\sigma_k+\sigma_j)t}\cos((\omega_{SSk}-\omega_{SSj})t+\theta_{SSk}-\alpha_{SSj})+\\\sum_{k=1}^{n}U_{SSk}I_{SSk}e^{-2\sigma_k t}\cos(\theta_{SSk}-\alpha_{SSk})\end{Bmatrix} \quad (13)$$

$$p_{SS1,2}(t)=\frac{3}{2}\begin{Bmatrix}U_0I_{SS1}e^{-\sigma_1 t}\cos((\omega_0-\omega_{SS1})t+\theta_0-\alpha_{SS1})+\\U_{SS1}I_0e^{-\sigma_1 t}\cos((\omega_0-\omega_{SS1})t+\alpha_0-\theta_{SS1})+\\U_0I_{SS2}e^{-\sigma_2 t}\cos((\omega_0-\omega_{SS2})t+\theta_0-\alpha_{SS2})+\\U_{SS2}I_0e^{-\sigma_2 t}\cos((\omega_0-\omega_{SS2})t+\alpha_0-\theta_{SS2})+\\U_{SS1}I_{SS2}e^{-(\sigma_1+\sigma_2)t}\cos((\omega_{SS2}-\omega_{SS1})t+\alpha_{SS2}-\theta_{SS1})+\\U_{SS2}I_{SS1}e^{-(\sigma_1+\sigma_2)t}\cos((\omega_{SS2}-\omega_{SS1})t+\theta_{SS2}-\alpha_{SS1})+\\U_{SS1}I_{SS1}e^{-2\sigma_1 t}\cos(\theta_{SS1}-\alpha_{SS1})+U_{SS2}I_{SS2}e^{-2\sigma_2 t}\cos(\theta_{SS2}-\alpha_{SS2})\end{Bmatrix} \quad (14)$$

Compared with the expression of SSO power with a single oscillation source, the power components, generated by the interaction between different oscillation frequency components, are added to the SSO power. Two oscillation sources with frequencies of ω_{SS1} and ω_{SS2} are taken as an example in (14).

Compared with (7), the AC component with a frequency of $(\omega_{SS2}-\omega_{SS1})$ is added to SSO power. Since the fundamental frequency voltage is much larger than oscillation frequency voltage, the AC components with frequencies of $(\omega_0-\omega_{SS1})$ and $(\omega_0-\omega_{SS2})$ are still the main components in SSO power. Therefore, the SSO power with multiple sources can be approximated by (15), equal to the sum of the SSO power generated by each oscillation source separately.

$$p_{SSn}(t)\approx\frac{3}{2}\begin{Bmatrix}\sum_{k=1}^{n}U_{SSk}I_0e^{-\sigma_k t}\cos((\omega_0-\omega_{SSk})t+\alpha_0-\theta_{SSk})+\\\sum_{k=1}^{n}U_0I_{SSk}e^{-\sigma_k t}\cos((\omega_0-\omega_{SSk})t+\theta_0-\alpha_{SSk})+\\\sum_{k=1}^{n}U_{SSk}I_{SSk}e^{-2\sigma_k t}\cos(\theta_{SSk}-\alpha_{SSk})\end{Bmatrix}=\sum_{k=1}^{n}p_{SSk}(t) \quad (15)$$

When a system with multiple oscillation sources is in an asymmetrical operating state, the conclusion for a single oscillation source is still applicable. The ratio of the supersynchronous component $(\omega_0+\omega_{SSk})$ to the subsynchronous component $(\omega_0-\omega_{SSk})$ does not exceed the three-phase voltage unbalance factor ε. The SSO power is mainly composed of subsynchronous components at the frequencies of $(\omega_0-\omega_{SSk})$.

IV. SSO Power Propagation Characteristics

When the network is complex, there will be multiple propagation paths for SSO power. The propagation mechanism of AC component in SSO power is the main concern. From the definition of SSO power in (7), the AC component contains two items $p_{SS\_AC1}(t)e^{-\sigma t}$ and $p_{SS\_AC2}(t)e^{-\sigma t}$. The two items' magnitudes are affected by different elements. If we can obtain the quantitative relationship between the two items, we will know the element mainly affecting the SSO power propagation. After that, by obtaining the shunt coefficients of $p_{SS\_AC1}(t)$ and $p_{SS\_AC2}(t)$ based on their dominant elements, the AC SSO power on each branch can be calculated. Thus, the SSO propagation characteristics in a system are clarified. This section studies the influencing elements and propagation paths of SSO power.

A. SSO power propagation influencing elements

By analyzing the system with a single oscillation source shown in Fig.2, the influencing elements of AC and DC components included in the SSO power are studied respectively.

(1) The influencing elements of AC power component

The AC component is the power fluctuation that causes harm to the power grid. Equation (7) shows that the magnitude of the AC component is determined by $U_{SS}I_0$ and U_0I_{SS}. Wind farm

output voltage U_0 and oscillation source voltage U_{SS} have small fluctuation ranges under different working conditions. Thus, I_0 and I_{SS} determine the magnitude of the AC power components. In the following qualitatively analysis of influencing elements, the damping σ are not included.

The fundamental current I_0 is proportional to the fundamental active power flow. The fundamental voltage U_0 does not change. So, I_0 is mainly related to the fundamental power flow. The subsynchronous current I_{SS} is analyzed next. The subsynchronous voltage drop on the lth branch is shown in (16).

$$\begin{aligned}\Delta u_{SS}(t) &= u_{SS}(t) - u_{lSS}(t) \\ &= U_{SS}\cos(\omega_{SS}t+\theta_{SS}) - U_{lSS}\cos(\omega_{SS}t+\theta_{lSS})\end{aligned} \tag{16}$$

The voltage magnitudes at two terminals of the branch U_{SS} and U_{lSS} are close. The magnitude is assumed to be U_{SS}, which is reasonable because the voltage drop on the line in the practical power system is small.

The magnitude of the voltage drop can be expressed by (17).

$$\Delta U_{SS} \approx 2U_{SS}\sin\left(\frac{\theta_{SS}-\theta_{lSS}}{2}\right) \tag{17}$$

Thus, the magnitude of the subsynchronous current can be expressed by (18).

$$I_{SS} \approx 2U_{SS}\sin\left(\frac{\theta_{SS}-\theta_{lSS}}{2}\right)\Big/\left|Z(\omega_{SS})\right| \tag{18}$$

Where $Z(\omega_{SS})$ is the impedance of RLC line at SSO frequency ω_{SS}. Equation (18) indicates that the magnitude of SSO current is mainly affected by line impedance.

From the above analysis, the magnitude $U_{SS}I_0$ of $p_{SS\_AC1}(t)$ is mainly affected by power flow. SSO power propagating in the branch will increase as the fundamental power flow in this branch increases. The magnitude U_0I_{SS} of $p_{SS\_AC2}(t)$ is mainly affected by line impedance. The smaller the line impedance is at ω_{SS}, i.e. the closer the line resonant frequency is to ω_{SS}, the more the SSO power propagates in the branch.

(2) The influencing elements of the DC power component

Equation (18) indicates that I_{SS} is mainly affected by line impedance. Therefore, $U_{SS}I_{SS}$ of the DC component in the SSO power is affected by line impedance.

In summary, the propagation of AC components is affected by both power flow and line impedance, but the propagation of DC component is only related to the line impedance.

B. Impact factor of SSO power propagation

This subsection compares the capabilities of these two elements influencing SSO power propagation. The impact factor of SSO power propagation is proposed to quantitatively determine which influencing element has a dominant impact under different operating conditions. The magnitude ratio of $p_{SS\_AC1}(t)$ to $p_{SS\_AC2}(t)$ in (7) is proportional to the ratio of line impedance at ω_{SS} to line impedance at ω_0, as shown in (19).

$$A_{SS1}=U_{SS}I_0e^{-\sigma t},\ A_{SS2}=U_0I_{SS}e^{-\sigma t},\ \frac{A_{SS1}}{A_{SS2}}=\frac{U_{SS}I_0}{U_0I_{SS}}\propto\frac{\left|Z(\omega_{SS})\right|}{\left|Z(\omega_0)\right|} \tag{19}$$

Therefore, the impact factor IF_{SS} of SSO power propagation is defined as the ratio of line impedance at ω_{SS} to line impedance at ω_0, as shown in (20).

$$IF_{SS}=\left|Z(\omega_{SS})\right|\Big/\left|Z(\omega_0)\right| \tag{20}$$

During the subsynchronous range from 2.5Hz to 50Hz, the frequency impedance characteristic of a RLC transmission line is shown in Fig.3. The lowest point of the curve is at line resonance frequency. When ω_{SS} is in the frequency range of green area, line impedance at ω_{SS} is bigger than that at ω_0. Otherwise, line impedance at ω_{SS} is smaller.

When line impedance at ω_{SS} is bigger than that at ω_0, IF_{SS} is greater than 1 and $p_{SS\_AC1}(t)$ is dominant in SSO power. In this situation, SSO power propagation is mainly affected by power flow. When the resonant frequency of the line is close to ω_{SS}, the line impedance at ω_{SS} is close to 0 and I_{SS} is relatively large. In this case, IF_{SS} is close to 0 and SSO power is mainly composed of $p_{SS\_AC2}(t)$. SSO power propagation is mainly affected by line impedance. The summary of the impact factor is in Table I.

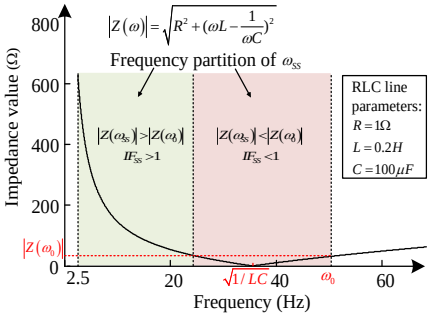

Fig.3 Frequency impedance characteristic of a RLC transmission line

TABLE I
THE IMPACT FACTOR OF SSO POWER PROPAGATION

Impact Factor	Line impedance	The SSO power magnitudes	The dominant influencing element
$IF_{SS}>1$	$\|Z(\omega_{SS})\|>\|Z(\omega_0)\|$	$A_{SS1}>A_{SS2}$	Power flow
$IF_{SS}<1$	$\|Z(\omega_{SS})\|<\|Z(\omega_0)\|$	$A_{SS1}<A_{SS2}$	Line impedance

C. Shunt coefficient of SSO power propagation

The shunt coefficient of SSO power propagation is proposed considering the aforementioned two influencing elements. The coefficient can quantitatively characterize SSO propagation path. In another word, the shunt coefficient of a branch is the ratio of the SSO power through this branch to the sum of SSO power through all branches. Each branch has its own shunt coefficient. The value of SSO power through a branch can be calculated by this coefficient. The propagation paths of the DC and AC components are studied as follows.

(1) The shunt coefficient of the DC component in SSO power

Since the propagation of DC component is determined by line impedance, the shunt coefficient of the DC component is defined in (21), where $Z_l(\omega_{SS})$ is the impedance of the lth branch at ω_{SS}.

$$KP_{dc}^{l}=I_{SS}^{l}\Big/\sum_{i=1}^{n}I_{SS}^{i}=\left|Z_l(\omega_{SS})\right|\Big/\sum_{i=1}^{n}\left|Z_i(\omega_{SS})\right| \tag{21}$$

(2) The shunt coefficient of the AC component in SSO power

From the previous analysis on the impact factor, the magnitude of $p_{SS\_AC1}(t)$ is determined by power flow. The magnitude of $p_{SS\_AC2}(t)$ is determined by line impedance. Therefore, shunt coefficients of these two can be expressed in (22). P^{l}_0 is the fundamental active power on the lth branch.

$$K_1^l = I_0^l \Big/ \sum_{i=1}^{n} I_0^i = P_0^l \Big/ \sum_{i=1}^{n} P_0^i, \quad K_2^l = I_{SS}^l \Big/ \sum_{i=1}^{n} I_{SS}^i = |Z_l(\omega_{SS})| \Big/ \sum_{i=1}^{n} |Z_i(\omega_{SS})| \quad (22)$$

The magnitudes A_1 and A_2 of $p_{SS\_AC1}(t)$ and $p_{SS\_AC2}(t)$ at PCC can be expressed by (23). The damping σ is not included because it will be cancelled in the calculation.

$$A_1 = U_{SS} I_0 = U_{SS} \sum_{i=1}^{n} I_0^i, \quad A_2 = U_0 I_{SS} = U_0 \sum_{i=1}^{n} I_{SS}^i \quad (23)$$

The phase difference between $p_{SS\_AC1}(t)$ and $p_{SS\_AC2}(t)$ in (7) is $(\theta_0 - \alpha_0) + (\theta_{SS} - \alpha_{SS})$. $(\theta_0 - \alpha_0)$ is the angle between the fundamental voltage and the fundamental current at PCC, i.e. the power factor angle ψ_0. $(\theta_{SS} - \alpha_{SS})$ is close to 90° because the transmission line is generally inductive. The magnitude of the AC power component through the lth branch can be gained by (24).

$$A^l{}_{SS\_AC} = \sqrt{\left(K_1^l A_1 - K_2^l A_2 \sin\psi_0^l\right)^2 + \left(K_2^l A_2 \cos\psi_0^l\right)^2} \quad (24)$$

Then, the shunt coefficient $KP^l{}_{ac}$ of the AC component in SSO power is defined as the ratio of the AC component through the lth branch to the sum of the AC components through all branches. The $KP^l{}_{ac}$ definition is shown in (25).

$$KP_{ac}^l = \frac{A^l{}_{SS\_AC}}{\sum_{i=1}^{n} A^i{}_{SS\_AC}} = \frac{\sqrt{\left(K_1^l A_1 - K_2^l A_2 \sin\psi_0^l\right)^2 + \left(K_2^l A_2 \cos\psi_0^l\right)^2}}{\sum_{i=1}^{n} \sqrt{\left(K_1^i A_1 - K_2^i A_2 \sin\psi_0^i\right)^2 + \left(K_2^i A_2 \cos\psi_0^i\right)^2}} \quad (25)$$

The calculation of shunt coefficient can reveal the propagation characteristics of different oscillation frequency components in the SSO power. The propagation path of DC component can be used in SSO source detection. The propagation path of AC component can guide SSO mitigation strategies.

D. *Propagation with multiple oscillation sources*

From (15), SSO power with multiple oscillation sources is approximated as the sum of the SSO power with each single oscillation source. The impact factors vary at different oscillation frequencies, so are the shunt coefficients. Therefore, by using the superposition theorem, we can study the propagation characteristics with multiple oscillation sources by studying each oscillation frequency component's propagation.

V. Case Studies

In this section, two representative systems are established to validate the proposed SSO power propagation characteristics. Time-domain simulations are built on PSCAD/EMTDC.

A. *Single oscillation source simulation*

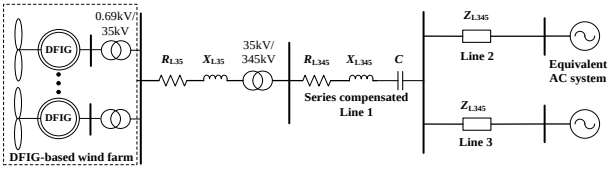

Fig.4 The system model of a DFIG-based wind farm connected to the grid through a series compensation line

Considering practical SSO events, a single oscillation source system model is shown in Fig.4. DFIGs are connected to the grid through 0.69kV/35kV transformers. The power from the wind farm is transmitted through a 35kV/345kV step-up transformer and a series-compensated line. After that, two lines with the same impedance are connected to two equivalent AC systems. The DFIG-based wind farm consists of 1000 identical DFIGs with a rated power of 1.5 MW. The impact of power flow and line impedance on SSO power propagation is studied. Besides, an asymmetrical system operation state is simulated.

(1) Impact of power flow ($IF_{SS} > 1$)

Lines 2 and 3 send 1000 MW and 500 MW of fundamental frequency active power respectively. The series compensation is installed on the transmission line at 10s. Then the SSO occurs in the system. In this case (IF_{SS} = 1.7), the line resonance frequency is away from the SSO frequency (ω_{SS} = 7Hz).

Fig.5(a) shows the phase A current of Line 1 and its WFFT spectrum result. Fig.5(b) shows the three-phase instantaneous active power and its WFFT spectrum result. The frequency of the subsynchronous component in the instantaneous active power and the frequency of the subsynchronous current complement each other, where the sum is equal to 50Hz. The power output from the wind farm propagates to Lines 2 and 3. After series compensation is installed, the power starts to oscillate and its oscillation amplitude increases gradually. From Fig.5(b), the SSO power at 43Hz ($\omega_0 - \omega_{SS}$) is propagating in the system. Line 2 transmits 51.8MW more SSO power than Line 3. The line that delivers more fundamental frequency active power transmits more SSO power. The shunt coefficients $KP^2{}_{ac}$ and $KP^3{}_{ac}$ of the two lines are calculated to be 0.66 and 0.34 by substituting system parameters into (25). The simulation results are 0.66 and 0.34, consistent with theoretical shunt coefficients $KP^2{}_{ac}$ and $KP^3{}_{ac}$.

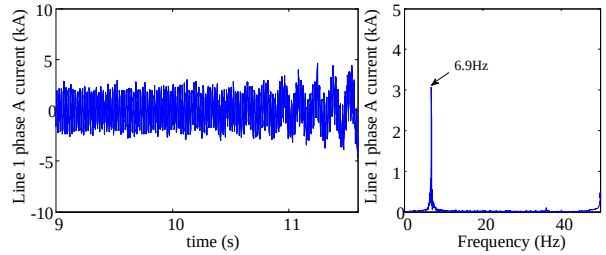

(a) Line 1 phase A current and its WFFT spectrum analysis

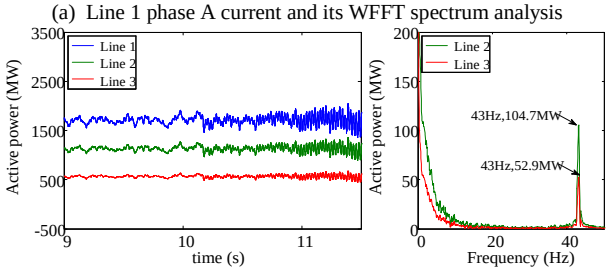

(b) Three-phase instantaneous active power and its WFFT spectrum analysis

Fig.5 Impact of power flow on SSO power with a single oscillation source

(2) Impact of line impedance characteristics ($IF_{SS} < 1$)

To study the impact of line impedance on SSO power propagation, the fundamental power flow is maintained the same. Line 3 installs a series capacitor and its resonant frequency becomes close to the SSO frequency and IF_{SS} = 0.1.

The simulation results are shown in Fig.6. Although Line 3 transmits 500MW less fundamental power than Line 2, the SSO power through Line 3 is 94.4MW more than that through Line 2. When the resonant frequency of Line 3 is close to the SSO

frequency, the impedance of Line 3 at the SSO frequency is much smaller than that at the fundamental frequency, where $Z(\omega_0)$ is 10.4 times bigger than $Z(\omega_{SS})$. In this case, the line impedance characteristic plays a leading role in SSO power propagation. The ratio of AC SSO power on Line 3 to the total AC SSO power of the two transmission lines is 0.83, consistent with the theoretical result KP^3_{ac}.

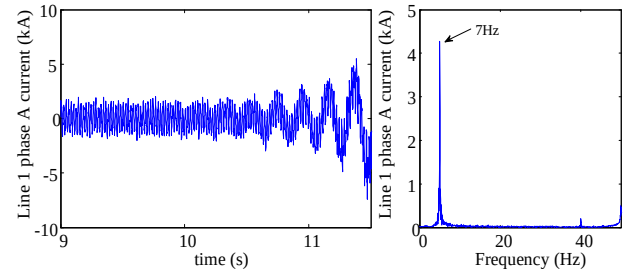

(a) Line 1 phase A current and its WFFT spectrum analysis

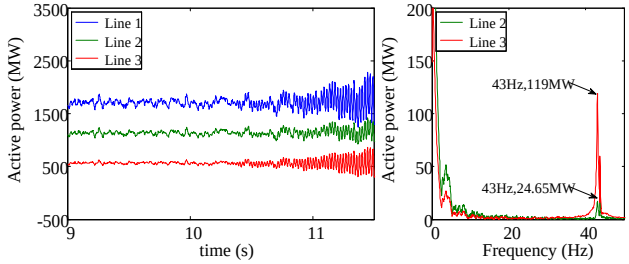

(b) Three-phase instantaneous active power and its WFFT spectrum analysis

Fig.6 Impact of line impedance on SSO power with a single oscillation source

(3) Influence of asymmetrical operation

The three-phase voltage is set to 10% unbalance by adjusting the three-phase load. The simulation results before and after the adjustment are shown in Fig.7. In addition to the power component with an oscillation frequency of 43Hz ($\omega_0 - \omega_{SS}$), there are also the two power components of 57 Hz ($\omega_0 + \omega_{SS}$) and 14Hz ($2\omega_{SS}$). The amplitude ratio of the 57 Hz power component to the 43Hz power component is close to 10%, which is consistent with the theoretical analysis.

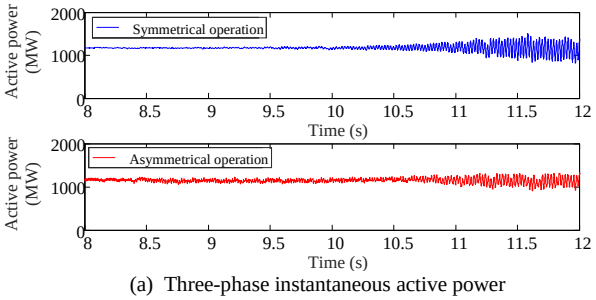

(a) Three-phase instantaneous active power

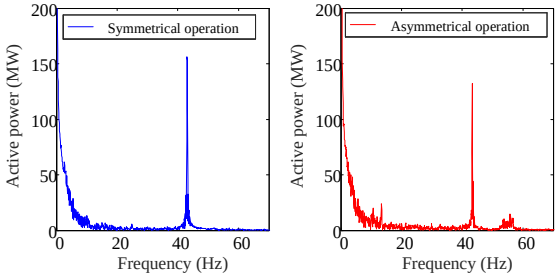

(b) WFFT spectrum analysis of the active power

Fig.7 Impact of asymmetrical operation on SSO power

B. Multiple oscillation sources simulation

Time-domain simulations are conducted on a system of two PMSG-based wind farms connected to a weak power grid, shown in Fig.8. Both wind farms contain 400 PMSGs with the rated power of 5MW. The PMSGs are connected to the 35kV bus through 0.69/35kV transformers. Then, the wind power is transmitted to the 345kV substation through the 35kV Line 1. After that, two transmission lines (Line 2 and Line 3) with the same impedance are connected to the AC systems.

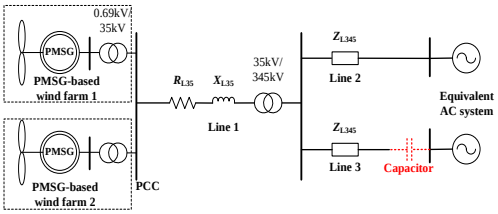

Fig.8 System model of a PMSG-based wind farm connected to a weak grid

(1) Influence of power flow ($IF_{SS} > 1$)

Line 2 and Line 3 are set to send 2300MW and 1700MW of fundamental frequency active power respectively. Two subsynchronous currents (ω_{SS1}=10Hz and ω_{SS2}=16Hz) are injected into the two wind farms respectively to excite the SSO at 10s. The impact factors of the two oscillation frequency components are both larger than 1 (IF_{SS1}=15.4 and IF_{SS2}=9.2).

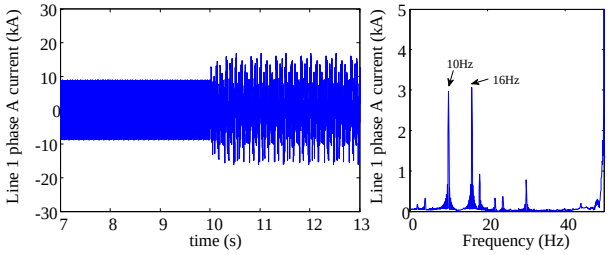

(a) Line 1 phase A current and its WFFT spectrum analysis

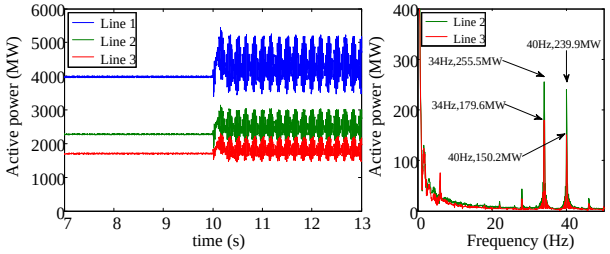

(b) Three-phase instantaneous active power and its WFFT spectrum analysis

Fig.9 Impact of power flow on SSO power with multiple oscillation sources

Fig.9 shows simulation results with two oscillation sources before and after the disturbance. The output of the active power on each line diverges rapidly and develops into an undamped oscillation. The subsynchronous active power mainly contains two components with oscillation frequencies of 34Hz and 40Hz. The frequencies of the oscillation power and those of the currents are complementary. By analyzing different oscillation frequency components, we can find that the propagations of 34Hz and 40Hz power components are both dominated by power flow. There are 600MW more fundamental frequency power flow, 75.9MW more 34Hz SSO power component, and 89.7MW more 40Hz SSO power component on Line 2. Two frequency power components' shunt coefficients vary because

line impedances and subsynchronous current amplitudes vary at different frequencies. Theoretical results for the different frequency power components through Line 3 are 0.41 (34Hz) and 0.39 (40Hz), consistent with simulation results.

(2) Influence of line impedance characteristics (IF_{SS} < 1)

In this case, the impact of line impedance characteristics on the SSO power is studied. The fundamental power flow is maintained the same and Line 3 installs a series capacitor and its resonant frequency is 10Hz. The impact factors of two oscillation frequency components are both smaller than 1 (IF_{SS1}=0.03 and IF_{SS2}=0.2, when ω_{SS1}=10Hz, ω_{SS2}=16Hz).

Simulation results in Fig.10 show that Line 3 transmits 64.8MW more SSO power component at 34Hz and 94.1MW more SSO power component at 40Hz than Line 2, while Line 3 transmits 600MW less fundamental power. It verifies that these two SSO power components are dominated by line impedance. Line 3's shunt coefficient theoretical results are 0.59 (34Hz) and 0.63 (40Hz), consistent with simulation results.

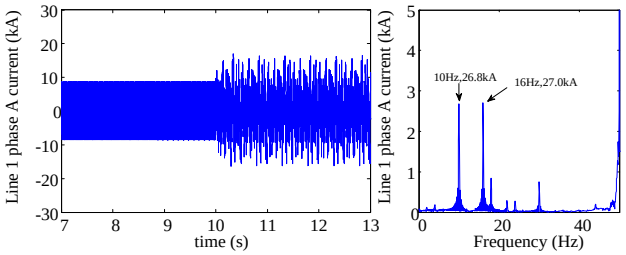

(a) Line 1 phase A current and its WFFT spectrum analysis

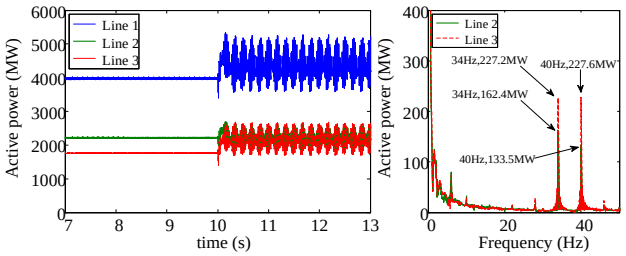

(b) Three-phase instantaneous active power and its WFFT spectrum analysis

Fig.10 Impact of line impedance on SSO power with multiple oscillation sources

C. Practical case verification

The theory in this paper is applied in a practical case as follows. In the northern area of Xinjiang, China, sustained power oscillations at subsynchronous frequency originated from direct-drive PMSG based wind farms and spread far to the external power grids. Because of the propagation of SSO power, the nearby turbogenerators were stimulated intense torsional vibration. The one-line diagram of this system is illustrated in Fig.11, which simplifies the main grid in Xinjiang to highlight the issue concerned [5].

As shown in Fig.11, PMSG based wind farms located in MWest, MEast and NMH are connected to SB substation through 220kV long-distance transmission line. Then the wind power is transmitted to Hami substation through 220kV double circuit lines, where the voltage is stepped up to 750kV. In 750 kV grid, there are two thermal power plants and a HVDC transmission line connected to the TS substation. Other parts of this grid are simplified to Gird A, B and C without showing their subordinate lower voltage grids.

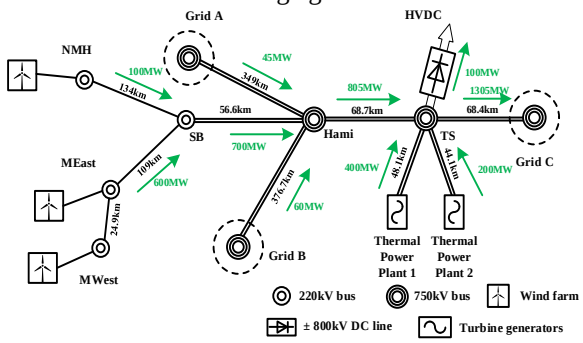

Fig.11 One-line diagram of the practical case in Xinjiang suffering SSO

Under a normal condition, the fundamental frequency power flow is shown in Fig.11. During a SSO event observed under this operation condition of the system, the oscillatory active power with a frequency of 26.95Hz started to diverge and soon entered in a state of sustained oscillation. According to the theory in this paper, the impact factor of the oscillation frequency is smaller than 1, because the transmission lines in this system have no series compensation. SSO power propagation in this practical case is mainly affected by line impedance.

Theoretical results of the shunt coefficient of each transmission line are listed in Table II. It shows that most of the SSO power propagated to the thermal power plants connected to TS. This is consistent with the real phenomenon that the turbine generators in this thermal power plants were stimulated intense torsional vibration.

TABLE II
THE SHUNT COEFFICIENTS OF SSO POWER PROPAGATION

Hami to Grid A	Hami to Grid B	Hami to TS	TS to HVDC
0.048	0.094	0.858	0.012
TS to Thermal power plant 1	TS to Thermal power plant 2	TS to Grid C	
0.517	**0.263**	0.208	

VI. CONCLUSION

This paper has presented a new definition of SSO power and revealed the SSO propagation characteristics by discussing the dominant influencing element and calculating the propagation paths. This paper has shown that SSO power contains subsynchronous components and DC component when the system is operating symmetrically. It also contains supersynchronous components in system asymmetrical operation. The propagation of AC components in the SSO power is affected by both fundamental frequency power flow and line impedance. The dominant influencing element is determined by the relationships between line impedances at oscillation and fundamental frequencies. The shunt coefficient is proposed to calculate the propagation path of the SSO power. Analysis with multiple oscillation sources indicates that the propagation paths of different frequency components in the SSO power are various in the same network. The correctness of the theoretical analyses is verified with both single oscillation source and multiple oscillation sources.

REFERENCES

[1] D. H. R. Suriyaarachchi, U. D. Annakkage, C. Karawita and D. A. Jacobson, "A procedure to study sub-synchronous interactions in wind integrated power systems," *IEEE Transactions on Power Systems*, vol. 28, no. 1, pp. 377-384, 2012.

[2] J. Li and X. Zhang, "Impact of increased wind power generation on subsynchronous resonance of turbine-generator units," *Journal of Modern Power Systems and Clean Energy*, vol. 4, no. 2, pp. 219-228, 2016.

[3] Y. Tang and R. Yu, "Impacts of large-scale wind power integration on subsynchronous resonance," in *2011 Asia-Pacific Power and Energy Engineering Conference*, IEEE, 2011, pp. 1-4.

[4] P. H. Huang, M. S. El Moursi, W. Xiao, J. L. Kirtley, "Subsynchronous resonance mitigation for series-compensated DFIG-based wind farm by using two-degree-of-freedom control strategy," *IEEE Transactions on Power Systems*, vol. 30, no. 3, pp. 1442-1454, 2014.

[5] H. Liu, X. Xie, J. He, T. Xu, Z. Yu, C. Wang and C. Zhang, "Subsynchronous interaction between direct-drive PMSG based wind farms and weak AC networks," *IEEE Transactions on Power Systems*, vol. 32, no. 6, pp. 4708-4720, 2017.

[6] A. E. Leon and J. A. Solsona, "Sub-synchronous interaction damping control for DFIG wind turbines," *IEEE Transactions on Power Systems*, vol. 30, no. 1, pp. 419-428, 2014.

[7] J. Adams, V. A. Pappu and A. Dixit, "Ercot experience screening for Sub-Synchronous Control Interaction in the vicinity of series capacitor banks," in *2012 IEEE Power and Energy Society General Meeting*, San Diego, CA, USA, New York: IEEE, 2012, pp. 1-5.

[8] X. Zhan, C. Liu and Z. Wang, "Analysis and control on Sub-synchronous oscillation (SSO) of HVDC transmission for large-scale permanent magnet synchronous generators (PMSG)-based wind farm integration," *The Journal of Engineering*, vol. 2019, no. 16, pp. 2440-2444, 2019.

[9] W. Liu, X. Xie, H. Liu and J. He, "Mechanism and characteristic analyses of subsynchronous oscillations caused by the interactions between direct-drive wind turbines and weak AC power systems," *The Journal of Engineering*, vol. 2017, no. 13, pp. 1651-1656, 2017.

[10] L. Fan, R. Kavasseri, Z. Miao and C. Zhu, "Modeling of DFIG-based wind farms for SSR analysis," *IEEE Transactions on Power Delivery*, vol. 25, no. 4, pp. 2073-2082, 2010.

[11] X. Xie, X. Zhang, H. K. Liu and H. Liu, "Characteristic analysis of subsynchronous resonance in practical wind farms connected to series-compensated transmissions," *IEEE Transactions on Energy Conversion*, 2017, 32(3): 1117-1126.

[12] W. Du, B. Ren, H. Wang and Y. Wang, "Comparison of methods to examine sub-synchronous oscillations caused by grid-connected wind turbine generators," *IEEE Transactions on Power Systems*, vol. 34, no. 6, pp. 4931-4943, 2019.

[13] Y. Li, L. Fan and Z. Miao, "Wind in Weak Grids: Low-Frequency Oscillations, Subsynchronous Oscillations, and Torsional Interactions," *IEEE Transactions on Power Systems*, vol. 35, no. 1, pp. 109-118, 2019.

[14] Y. Gong, Q. Huang, J. Li and D. Cai, "Analysis on Oscillation Propagation Characteristics based on Impedance Model," in *2019 IEEE Innovative Smart Grid Technologies-Asia (ISGT Asia)*, IEEE, 2019, pp. 1226-1229.

[15] B. Gao, Y. Wang, W. Xu and G. Yang, "Identifying and Ranking Sources of SSR Based on the Concept of Subsynchronous Power," *IEEE Transactions on Power Delivery*, vol. 35, no. 1, pp. 258-268, Feb. 2020.

[16] X. Xie, Y. Zhan, J. Shair, Z. Ka and X. Chang, "Identifying the Source of Subsynchronous Control Interaction via Wide-Area Monitoring of Sub/Super-Synchronous Power Flows," *IEEE Transactions on Power Delivery*, vol. 35, no,5, pp. 2177-2185, 2020.

[17] H. Akagi, Y. Kanazawa and A. Nabae, "Instantaneous reactive power compensators comprising switching devices without energy storage components," *IEEE Transactions on industry applications*, vol. IA-20, no. 3, pp. 625-630, May 1984.

[18] E. H. Watanabe, R. M. Stephan and M. Aredes, "New concepts of instantaneous active and reactive powers in electrical systems with generic loads," *IEEE Transactions on Power Delivery*, vol. 8, no. 2, pp. 697-703, April 1993.

[19] Z. Wen, S. Peng, J. Yang, J. Deng, H. He and T. Wang, "Analysis of the Propagation Characteristic of Subsynchronous Oscillation in Wind Integrated Power System," Energies, vol. 12, no. 6, pp. 1081, 2019.

[20] P. Zhang, P. Xu and T. Bi, "Analysis of subsynchronous current propagation path of subsynchronous oscillation induced by renewable energy integrated to the power grid," *The Journal of Engineering*, vol. 2017, no. 13, pp. 2449-2454, 2017.

[21] L. Chen, Y. Min and W. Hu, "An energy-based method for location of power system oscillation source," *IEEE Transactions on Power Systems*, vol. 28, no.12, pp.828-836, 2012.

Na Yang received the B.S. degree from Shanghai Jiao Tong University, Shanghai, China, in 2018. She is currently working toward the M.S. degree in electrical engineering at Shanghai Jiao Tong University, Shanghai, China. Her major research interests include dynamics, simulation and control of electromechanical interactions in power systems.

Wenda Ma received the B.S. and M.S. degrees from Shanghai Jiao Tong University, Shanghai, China, in 2017 and 2020, respectively. His major research interests include dynamics, simulation and control of electromechanical interactions in power systems.

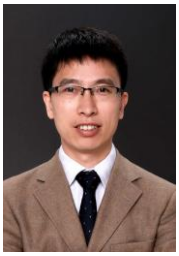

Xitian Wang (M'02) received the B.E. and Ph.D. degrees in power engineering from Harbin Institute of Technology, Harbin, China, in 1995 and 2001, respectively. Currently, he is an Associate Professor in the Department of Electrical Engineering, Shanghai Jiao Tong University, Shanghai, China. His major research interests include dynamics, simulation and control of electromechanical interactions in power systems.

Da Xie (M'02-SM'19) received the B.S. degree from Shanghai Jiao Tong University, Shanghai, China, in 1991; the M.S. degree from Harbin Institute of Technology, Harbin, China, in 1996; and the Ph.D. degree from Shanghai Jiao Tong University in 1999. He is currently a Professor with the Department of Electrical Engineering, Shanghai Jiao Tong University. His major research interests include multi-vector energy system, electrical system simulation, power electronic equipment, and smart grid.

Chenghong Gu (M'14) received the B.S. degree in electrical engineering from Shanghai University of Electric Power, Shanghai, China, in 2003, the M.S. degree in electrical engineering from Shanghai Jiao Tong University, Shanghai, in 2007, and the Ph.D. degree from the University of Bath, Bath, UK, in 2010. He is currently a Lecturer and EPSRC Fellow with the Department of Electronic and Electrical Engineering, University of Bath. His major research interests include multi-vector energy system, smart grid, and power economics.